Liquid Crystals
Publication details, including instructions for authors and subscription information:
http://www.informaworld.com/smpp/title~content=t713926090

Computer simulation of the homeotropic to planar transition in cholesteric liquid crystals

P. Watson[a]; J. E. Anderson[a]; V. Sergan[a]; P. J. Bos[a]
[a] Liquid Crystal Institute and Chemical Physics Interdisciplinary Program, Kent State University, Kent, OH 44242, USA,

Online publication date: 06 August 2010

To cite this Article Watson, P. , Anderson, J. E. , Sergan, V. and Bos, P. J.(2001) 'Computer simulation of the homeotropic to planar transition in cholesteric liquid crystals', Liquid Crystals, 28: 1, 1 — 15
To link to this Article: DOI: 10.1080/02678290010004984
URL: http://dx.doi.org/10.1080/02678290010004984

LIQUID CRYSTALS, 2001, VOL. 28, NO. 1, 1–15

Computer simulation of the homeotropic to planar transition in cholesteric liquid crystals

P. WATSON, J. E. ANDERSON*, V. SERGAN and P. J. BOS
Liquid Crystal Institute and Chemical Physics Interdisciplinary Program,
Kent State University, Kent, OH 44242, USA

(*Received 24 November 1999; in final form 25 May 2000; accepted 25 May 2000*)

The transition from the homeotropic to the planar state in cholesteric liquid crystal displays is investigated through computer simulation. The simulation reproduces the observed relaxation from the homeotropic state to the long pitch transient planar state. The simulation also agrees with the suggestion that the transition from the transient planar state to the planar state proceeds through a bulk modulation resulting in folding and buckling of cholesteric layers without introduction of defect cores. The model obtained agrees well with earlier experimental observations showing that the process includes a tilting of cholesteric helices, and that the surface plays only a minor role in the relaxation process.

1. Introduction

In cholesteric liquid crystal displays that reflect visible light [1], the transformation from the field-induced homeotropic (H) state to the reflecting planar (P) state is known to proceed via a metastable transient planar (TP) state with a cholesteric pitch significantly longer than the equilibrium pitch [2]. Yang and Lu [3] have explained that when the applied field is removed from the H state, the TP state is established through a one-dimensional conical relaxation. A longer pitch is formed because at the beginning of the relaxation, when the liquid crystal tilt angle is close to zero (nearly homeotropic), the Frank–Oseen free energy is locally minimized by a pitch that is equal to $P_0(K_{33}/K_{22})$, where P_0 is the intrinsic material pitch, and K_{33} and K_{22} are the bend and twist elastic constants, respectively. In virtually all chiral nematic materials, K_{33} is significantly greater than K_{22}. When the material begins twisting to reduce the high free energy of the homeotropic state, it soon becomes locked into a pitch somewhat longer than the intrinsic pitch, and a transient planar state is observed [3]. The TP state is simple to observe experimentally, and occurs regardless of boundary conditions [4].

2. Previous experimental findings

In earlier studies we investigated a simple cholesteric liquid crystal system. This was discussed in our previous work [7], and consisted of a 15 μm cell with rubbed planar surfaces, filled with a mixture of E. Merck liquid crystal ZLI 4792 and 3% CB15 chiral additive. This mixture resulted in a d/P (cell thickness over pitch) ratio for the cell of about 2.85.

Photomicrographic evidence suggested that the cell relaxed to a TP state with 1 twist in about 15 ms [7]. It remained in that state for about 200 ms, after which a bulk modulation with a striped appearance began to distort the texture (see figure 1). The wavelength of the modulation was measured to be 15.6 μm. Over the next 100 ms, the modulation became more pronounced, until

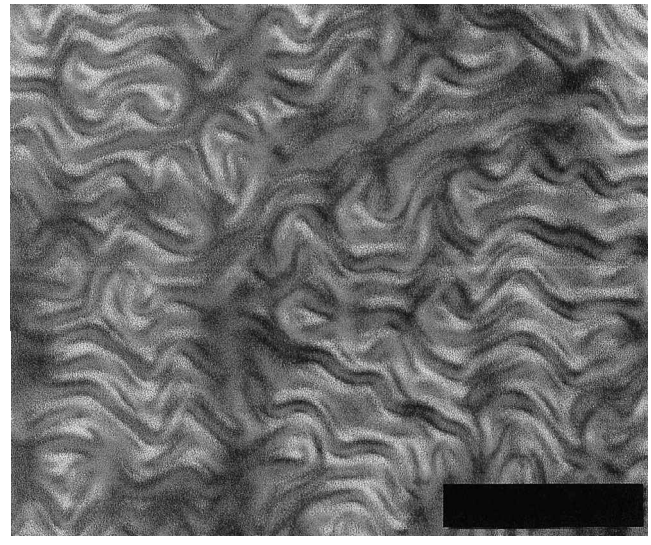

Figure 1. Photomicrograph of striped texture occurring during the TP to P transition in a simple cholesteric system. The black bar is 50 μm long.

* Author for correspondence; e-mail: janderson@hanaoh.com

Liquid Crystals ISSN 0267-8292 print/ISSN 1366-5855 online © 2001 Taylor & Francis Ltd
http://www.tandf.co.uk/journals
DOI: 10.1080/02678290010004984

the equilibrium texture was seen to appear between stripes. Stripes grouped into pairs, allowing larger regions of equilibrium texture to form. Eventually, the stripes were seen to disappear through continued grouping into pairs, as well as through shrinking due to defect motion in the third dimension. Because of the appearance and dimensions of these stripes, we proposed that they had a similar structure to those seen in a Helfrich deformation.

3. Experiment

In order to characterize the homeotropic to planar relaxation for a cholesteric liquid crystal cell reflecting visible light, a second cholesteric system was chosen. This system was reported in our previous work investigating the relaxation from H to FC [11]. It consists of two 5 μm cells filled with a mixture of E. Merck liquid crystal MLC 6080 and CB15 chiral additive in a 60:40 ratio by weight. The cell thickness to equilibrium pitch ratio for this system is $d/P = 13.9$. Cells with planar (rubbed DuPont 2555 polyimide) and homeotropic (Aldrich, octadecyltrichlorosilane) surface alignments were used. In order to characterize the director changes in the homeotropic to planar process, we chose to use capacitance measurements as initial indicator.

Cell capacitance was chosen because it is fairly simple to measure reproducibly in the laboratory, and can easily be determined from calculated director configurations. In order to measure changes in capacitance with a time resolution of better than 0.1 ms, Huang developed a technique in which an a.c. square wave voltage V_A is applied across a known capacitor C_0 and an unknown capacitor C_U in series [12]. We employed this method in analysing cholesteric liquid crystal samples. The value of the known capacitor was nominally 0.455 μF. For our applied voltage, a square wave signal generated by a National Instruments DAQ card using Electro-Optic Measurements [13] software developed at Kent State University was employed. The square wave was routed through a $1\times$–$10\times$ linear amplifier, and both V_A and V_0, the voltage across the know capacitor, were monitored using a Tektronix digitizing oscilloscope.

In addition to capacitance measurements, we used an optical retro-reflection technique described in previous work [4] to analyse the changes in pitch and helical axis distribution of this system. The apparatus for such measurements involves a white light source with a monochromator, a series of lenses and mirrors, and a photodiode detector. The system is designed such that only light reflected back along the incident light direction within a small cone will be detected. Geometrical measurements of the beam divergence suggest that the incident light cone is less than 5°, and measurements of reflections from a mirror placed in the cell holder and rotated suggest that the angular range of light acceptance of the optics is about 2°. We will consider the precision of the apparatus to be somewhere between these values. The reflection at each wavelength is recorded as a function of time after removal of the voltage from the sample. The data for all wavelengths between 375 and 1100 nm (in 25 nm increments) is fitted together to form a three-dimensional surface showing the reflection at various times in the relaxation process. The cell is tipped at various angles away from the incident light in order to allow for determination of the presence of cholesteric helices at angles away from the cell normal direction.

4. Experimental results and analysis

Plots of capacitance vs. time from the homeotropic to planar relaxation for cells with homeotropic and planar surfaces may be seen in figure 2. Note how, in both cases, the cell is initially in a configuration with a high capacitance. As time progresses, the liquid crystal transforms to a state with a much lower capacitance. This is then followed by a small increase in the capacitance of the system. This is consistent with the liquid crystal dropping from the H state to the TP state, and a subsequent distortion of the transient planar as the equilibrium planar pitch is formed. At longer time scales not shown on this graph, the capacitance in the cell with planar surfaces is seen to decrease gradually as the P state becomes more ordered. Based on measured values of capacitance in the H and perfect P states, the dielectric constants of the material were determined to be 5.5 for $\varepsilon_\perp$, and 14.3 for $\varepsilon_\parallel$.

A three-dimensional plot of data for the retroreflection analysis of the cell with the planar alignment at an incident angle of 5° is shown in figure 3. The vertical

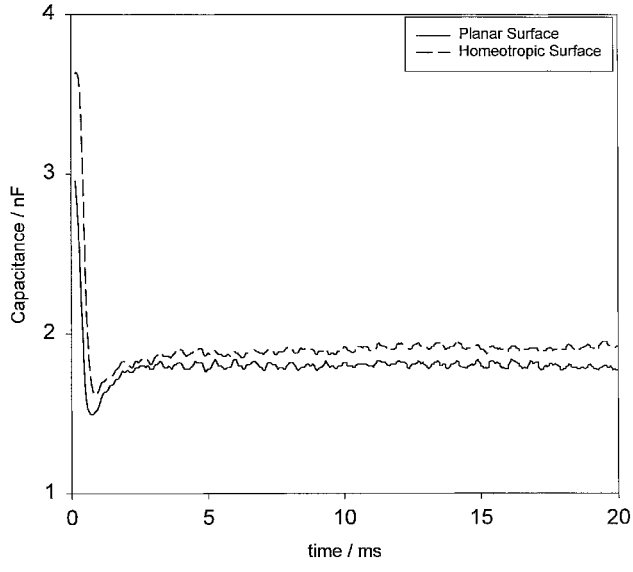

Figure 2. Experimental plot of capacitance vs. time for cells with different surfaces.

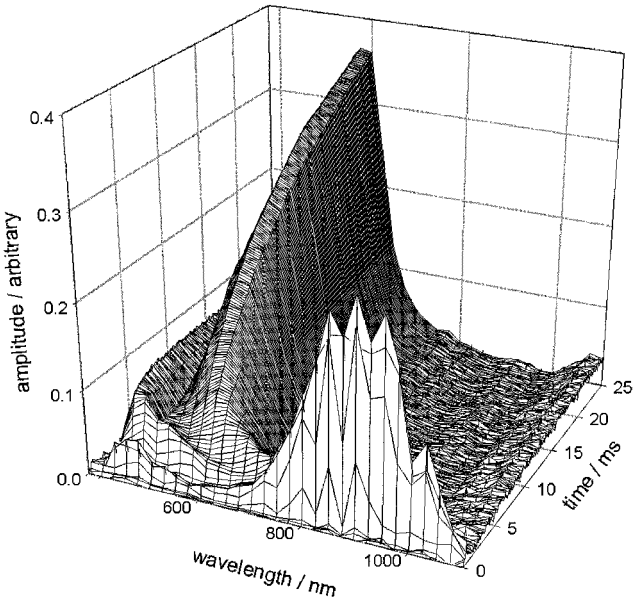

Figure 3. Experimental retroreflection data for cell with planar surfaces.

axis corresponds to reflected intensity (the normalized signal from the photodiode), while the two horizontal axes correspond to wavelength and time. About 1 ms into the relaxation process, a strong peak appears toward the long wavelength side of the figure, representing a bright reflection at about 1000 nm from the TP structure. As time progresses, this peak diminishes and the equilibrium planar peak appears and grows at about 600 nm. A similar plot corresponding to relaxation in the cell with homeotropic surfaces is shown in figure 4. Note that the primary features of the two plots are the same, although the amplitudes are significantly different. We have previously reported similar results for cells with a different nematic host material [4].

A plot of the wavelength of maximum reflection vs. time for the two cells may be seen in figure 5. The equilibrium wavelength is achieved in approximately 5 ms independent of surface. To see changes in the helical axis distribution (as in [4]), the reflected intensity integrated over all measured wavelengths at various times in the relaxation as a function of the angle of incidence α is shown for the planar and homeotropic surfaces in figure 6 (*a*) and 6 (*b*), respectively. Not shown is the data at angles less than 5°, where specular reflection overwhelms the desired signal. Note how the TP reflection (at about 1 ms) at small angles is somewhat brighter than that at larger angles. During the transition time (3 ms), the reflected intensity takes on a much wider angular distribution. As the system progresses into the P state (25 ms), the distribution for the planar cell becomes somewhat peaked at small angles, while that of the silane cell remains largely flat.

5. Simulation technique

For our modelling of the liquid crystal director, we used the same technique as discussed in a previous publication concerning the H to FC transition in cholesteric liquid crystals [11]. The expression for the free energy density of a liquid crystal system in terms of the director, **n**, is given by equation (1) [14].

The transformation from TP to P, however, has not been so well understood. Early papers, without attempting to understand the process, referred to the

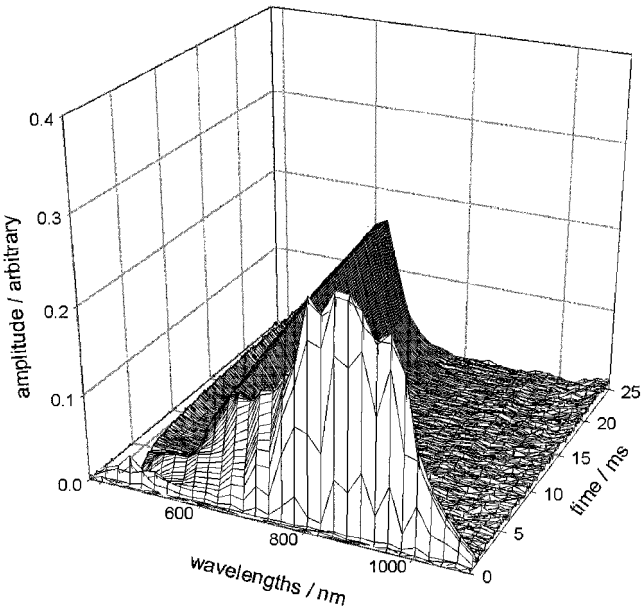

Figure 4. Experimental retroreflection data for cell with homeotropic surfaces.

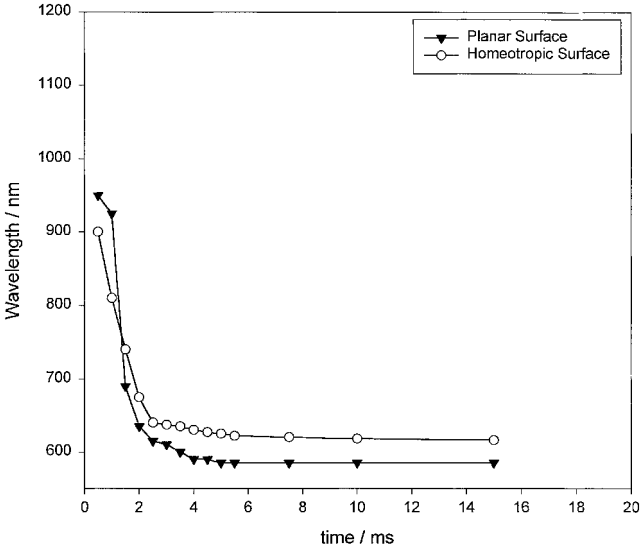

Figure 5. Experimental plot of wavelength of maximum reflection vs. time for cells with different surfaces.

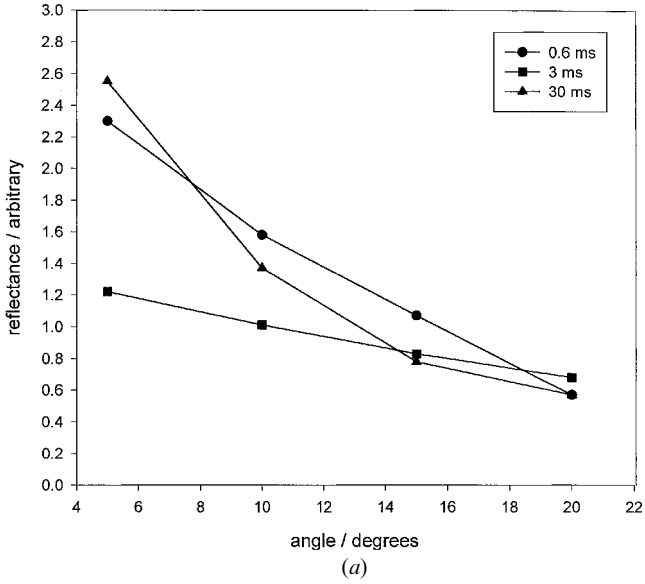

(*a*)

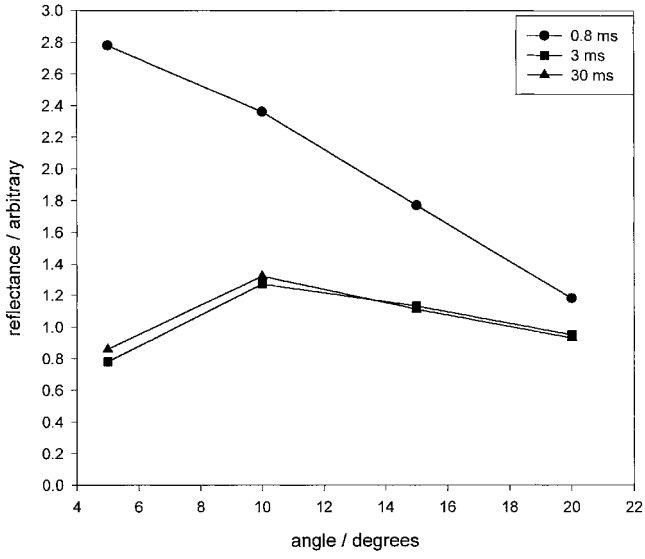

(*b*)

Figure 6. (*a*) The intensity of retro-reflection as a function of incidence angle at various times in the transition for the planar cell. (*b*) The intensity of retro-reflection as a function of incidence angle at various times in the transition for the silane cell.

transition simply as a 'rapid passage' [5]. Because the transition involves a change in twist, it has long been assumed that it involved a nucleation and diffusion process in which a small region of equilibrium P formed, separated from TP by a defect wall, and subsequently grew because it has a lower free energy than TP [3]. However, such a nucleation and growth process has not been observed in experiment.

In previous experimental work, we determined that during the transformation from TP to P, the angular distribution of reflecting cholesteric helices becomes quite large [4]. That is, the average cholesteric helical axis tilts away from the cell-normal direction as TP disappears and P forms. We also observed that the system, which is uniformly twisted throughout the cell in TP, becomes divided into domains as the transformation to P begins [4]. As the process continues, the domains grow and combine until an equilibrium condition is reached. The size of domains in the final state is related to the surface treatment [6], as is the helical axis distribution [4].

In order to determine the nature of the transition on a microscopic level, we observed the dynamics of related cholesteric systems with somewhat longer pitch [7]. We observed that the transformation from TP to P in these systems involved a bulk modulation that appeared similar to a Helfrich–Hurault stripe deformation [8–10]. The deformation appeared to be two-dimensional in nature. For samples with a very low number of twists, the stripe deformation was periodic approximately perpendicular to the rubbing direction. For samples with a greater degree of twist, the direction of periodicity was decoupled from the rubbing direction, and the stripes, though visible, were not as directionally ordered [7]. The modulation was seen to increase in amplitude with time, after which regions of equilibrium planar became visible between the stripes.

In related studies, we found through computer simulation and experimental verification that the related relaxation from H to the focal-conic (FC) state occurs through formation of a TP state, followed by a bulk modulation similar to a Helfrich transition [11]. We will now investigate the transformation to the planar state, including the nature of the stripe formation as well as the general transition from TP to P, using experimental techniques as well as two-dimensional Euler–Lagrange computer modelling techniques.

$$f = \frac{1}{2}K_{11}(\nabla \quad \mathbf{n})^2 + \frac{1}{2}K_{22}(\mathbf{n} \quad \nabla \times \mathbf{n} + q_0)^2 + \frac{1}{2}K_{33}|(\mathbf{n} \times \nabla \times \mathbf{n})|^2 - \frac{1}{2}\mathbf{D} \quad \mathbf{E} \tag{1}$$

where, K_{11}, K_{22}, and K_{33} are the elastic constants for splay, twist and bend, respectively, $\mathbf{D}$ is the electric displacement and $\mathbf{E}$ is the electric field.

Ignoring material flow the dynamics of the director reorientation can be calculated by setting the functional derivatives of the free energy density with respect to each director component (the elastic torque) equal to the rotational torque on that component as shown in equation (2) [15].

$$\gamma_1 \frac{\mathrm{d}n_i}{\mathrm{d}t} = -\frac{\delta f}{\delta n_i} + \lambda n_i, \quad i = x, y, z \tag{2}$$

where γ_1 is the rotational viscosity. In two dimensions,

$$\frac{\delta f}{\delta n_i} = \frac{\partial f}{\partial n_i} - \frac{\mathrm{d}}{\mathrm{d}x}\left(\frac{\partial f}{\partial \frac{\mathrm{d}n_i}{\mathrm{d}x}}\right) - \frac{\mathrm{d}}{\mathrm{d}z}\left(\frac{\partial f}{\partial \frac{\mathrm{d}n_i}{\mathrm{d}z}}\right), \quad i = x, y, z. \tag{3}$$

In equation (2), the Lagrange multiplier, λ, is used to maintain the unit length of the director. However, we cannot simultaneously solve this equation for the Lagrange multiplier and a numerical update formula for n_i. Therefore, the λ term is dropped and $\mathbf{n}$ is renormalized to have unit length after each time step, i.e. each director component is divided by the total length [16].

In our calculations, we assume that the starting point corresponds to a time shortly after the voltage has been removed; thus the voltage is assumed to be zero over the entire grid at all times, and is not taken into account. In order to calculate dynamics of the system, the new director field on the entire computational grid must be calculated before any variables are updated. Note that this model does not take into account flow effects or effects of ionic contaminants.

The effects we are trying to simulate in this study have been observed to be fundamentally two-dimensional in nature. In order for these two-dimensional effects to occur, it is necessary that some randomness be included in the system to allow the modulations that are observed to take place. If the initial homeotropic director configuration used in simulation is exactly $\mathbf{n} = (0, 0, 1)$ everywhere, we have found the calculation to relax to a metastable TP state that mathematically has only one-dimensional spatial dependences. To ensure that the director does not become stuck in a mathematically balanced state, we have included some random noise in the starting conditions for both systems. The initial director configurations were modified from pure homeotropic by first setting the director components n_x and n_y to random numbers between -0.05 and $+0.05$, then, using the relation $n_z = (1 - n_x^2 - n_y^2)^{1/2}$ (derived from the unit length of the director), to determine n_z. This results in an average deviation from the H state of roughly 1.4°. We have found, however, that the amplitude of this initial noise has very little effect on the outcome of the calculations or on intermediate states. As long as some amount of numerical noise is added to the initial homeotropic director configuration, the calculation will not end in a metastable state, but will proceed toward an equilibrium configuration.

6. Simulation of a simple cholesteric system

Calculations for the simple long pitch cholesteric system described in § 2 were based on a two-dimensional calculation grid of dimensions 208×125 in the x and z dimensions, respectively, with the x-axis parallel to the substrates and the z-axis perpendicular. The lattice dimensions were set such that the horizontal size of the grid was 25 μm, while the vertical size (cell gap) was 15 μm. Each lattice point thus represented a rectangle of dimensions 0.120 μm wide by 0.076 μm tall. Fixed homogeneous boundary conditions were assumed with a 5° pretilt. Because of the low concentration of chiral additive used in this system, the elastic constants and dielectric anisotropy of the host (ZLI 4792) were used in the calculation.

The simulation technique used here does not allow for changes in the scalar order parameter, which would allow defects to form. However, we have found that the free energy density for the simple low d/P system was always orders of magnitude lower than that required to form defects [11].

The simulation of the relaxation process from the homeotropic state to the transient planar state is shown in figure 7. In this sequence of pictures, the director at a lattice point is represented as a cylinder. The orientation of the cylinder indicates the average molecular orientation at the point in space associated with that lattice point. The cylinders are drawn as non-polar to represent the non-polar nature of the cholesteric phase. The drawings in this figure are down-sampled in order to improve viewability.

In the initial stages of the relaxation to TP, the director is seen to be in the H state, figure 7 (*a*). As time progresses, the director moves away from the cell-normal direction and into the plane of the cell, figures 7 (*b*, *c*). As expected, the director acquires a TP state with one full 360° twist, figure 7 (*d*).

As can be seen in figure 8, a modulation grows in the director configuration, initially with a sinusoidal appearance, (*a*). The modulation increased in amplitude (*b*) as the simulation progressed. The modulation at this time no longer has a sinusoidal appearance, but rather appears to exhibit 'fingers' which grow from the surfaces in a spatially alternating fashion. In (*c*–*e*), it may be seen that the ends of the 'fingers' mushroom out horizontally. The symmetry of the structures decays somewhat (*f*), and eventually the ends overlap each other (*g*–*i*). Note that this results in small tilted regions of the equilibrium pitch (3 twists). With increased time (*j*, *k*) the equilibrium pitch regions increased in size, agreeing well with the experimentally observed transition process.

7. Simulation of reflective display dynamics

To include the effect of the large proportion (40%) of chiral additive (CB15 from E. Merck) in the system on the elastic constants, we followed the report of Fedak *et al.* [17] to estimate the elastic constants in our system.

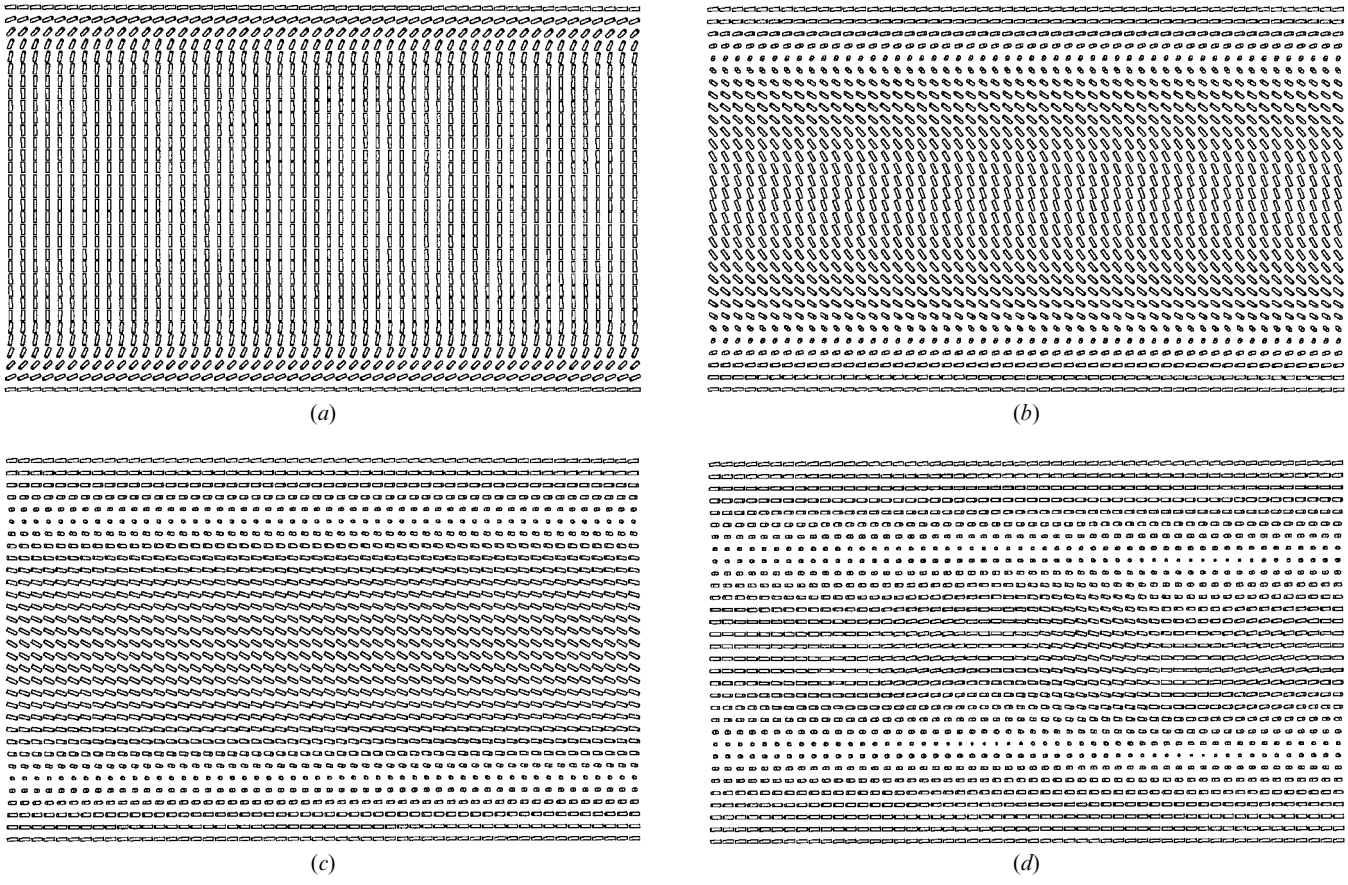

Figure 7. Simulated director configurations in relaxation from the homeotropic state to the transient planar state in a simple cholesteric system. These pictures represent a side view of the cell, with the top of the picture as the top substrate. Times are (*a*) 10 ms, (*b*) 50 ms, (*c*) 100 ms, (*d*) 400 ms.

These authors experimentally measured the elastic constants of a mixture as a function of weight % when both enantiomers of CB15 were added to a nematic host. The authors found a reduction of about 61.5%, 58.8% and 48.6% for K_{11}, K_{22} and K_{33}, respectively. We can include this effect by reducing the elastic constants of our system by these same percentages. For this study, we used MLC 6080 from E. Merck as the nematic host. We chose this material for its large birefringence ($\Delta n = 0.2024$) and low viscosity ($\gamma_1 \approx 0.133$ Pa s). The values of the elastic constants for our system were thus adjusted from 14.4, 7.1, and 19.1 pN to 8.86, 4.17 and 9.28 pN for K_{11}, K_{22} and K_{33} respectively. In previous work [12], we have found that these modifications to the material parameters have matched reasonably closely the observed experimental quantities.

In order to simulate the dynamics accurately, knowledge of the rotational viscosity γ_1 of the material is needed. It is expected that the addition of 40% CB15 will significantly alter the rotational viscosity. Several techniques were employed to determine this quantity. First, the relaxation time from the homeotropic to the transient planar state was chosen as a benchmark for determining this quantity. This time was chosen because the relaxation to the transient planar state is essentially one-dimensional in nature. Experimentally it was found that the lowest capacitance for the cell with planar alignment was achieved in about 0.75 ms. This corresponds to the time for the transient planar state to form. Using Berreman's BACKFG one-dimensional director simulation [18] and comparing the time taken to reach the minimum capacitance to experiment, yields a rotational viscosity of 0.033 Pa s. Using the multi-dimensional simulation program discussed above (but modified to allow only one-dimensional spatial dependences) resulted in a nearly identical value. However, the experimental minimum in capacitance in the TP state was measurably greater than $\varepsilon_\perp$, suggesting that some two-dimensional modulation effects take place before the transient planar state is fully achieved. Thus, we must use the minimum capacitance from a true two-dimensional calculation to determine the viscosity. The rotational viscosity obtained

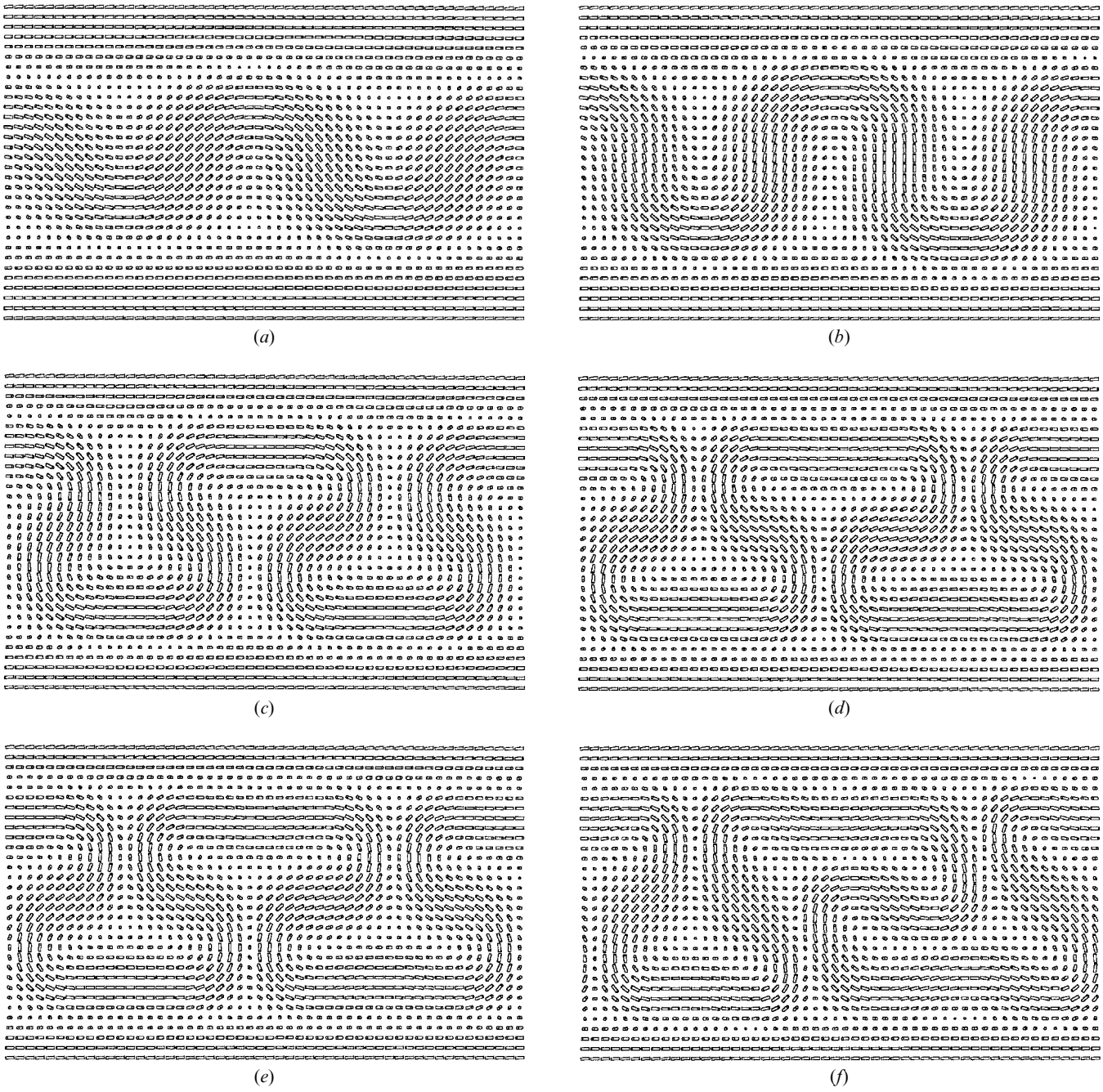

Figure 8. Simulated director configurations in relaxation from the transient planar state to the planar state in a simple cholesteric system after addition of a sinusoidal modulation. These pictures represent a side view of the cell, with the top of the picture as the top substrate. Times are (*a*) 600 ms, (*b*) 700 ms, (*c*) 800 ms, (*d*) 900 ms, (*e*) 1400 ms, (*f*) 1600 ms, (*g*) 1700 ms, (*h*) 1800 ms, (*i*) 1900 ms, (*j*) 2000 ms, (*k*) 2600 ms.

by setting the time of capacitance minima from the experiment and from preliminary two-dimensional simulations equal is 0.04 Pa s. We chose to use this value for the simulations. We also found this value to agree well with experiment for the H to FC transition [11].

Again, because of the simulation method employed here, no defects could form in the calculation. As in the low d/P system, the free energy density of the high d/P system was always at least a factor of 5 lower than that needed to form a defect [11].

The calculation lattice for this simulation was defined as a $5\,\mu m \times 5\,\mu m$ square, with 197 lattice points in each dimension. The surface conditions were set with a 3.75° pretilt and anti-parallel rubbing conditions for the cell

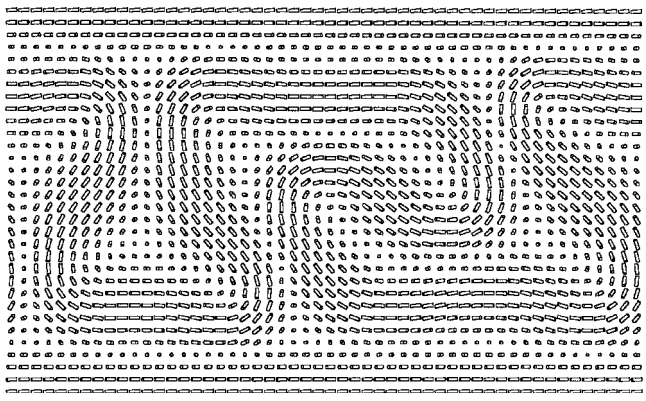

(*g*)

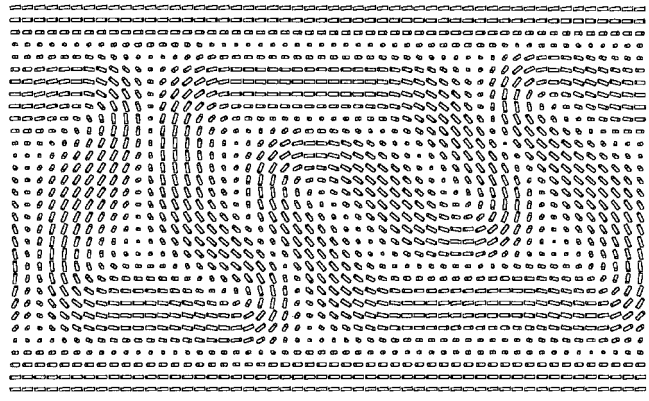

(*h*)

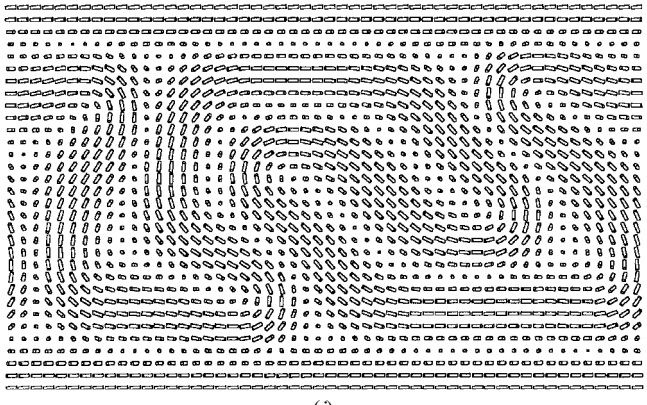

(*i*)

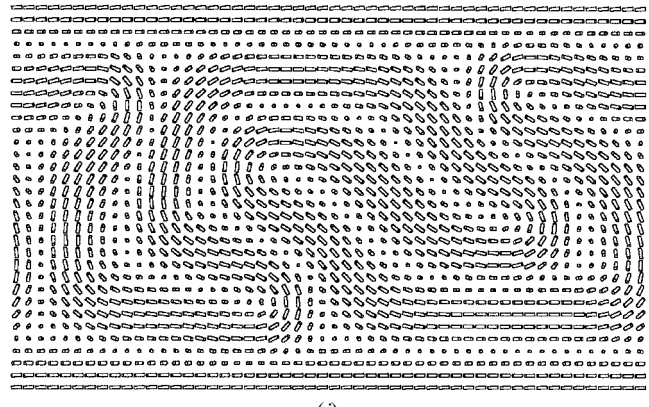

(*j*)

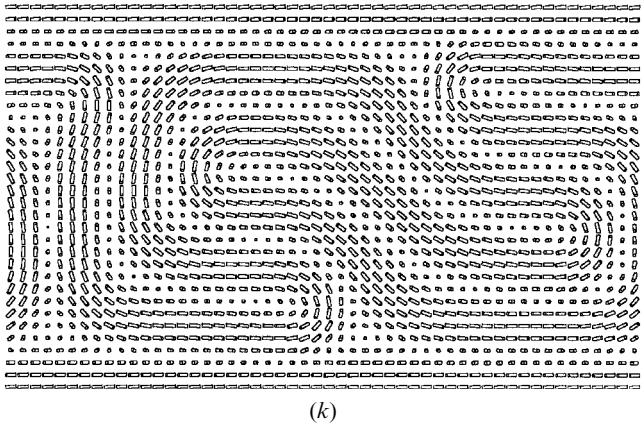

(*k*)

Figure 8. (*Continued.*)

with a planar surface, and 90° for the homeotropic cell. The initial configuration for the planar cell may be seen in figure 9 (*a*). As expected, the material is seen to relax quickly to a TP state with about six or seven twists (*b*) in about 0.8 ms. This TP state quickly becomes disturbed by a spatial oscillation of the layer structure (*c*). The magnitude of this modulation increases over time (*d–f*), and layers are seen to fold over onto themselves, resulting in a more twisted structure. As time progresses, regions of equilibrium pitch are seen to grow, and to align their helical axes along the cell-normal direction. Figure 10 shows a close-up of one area near the bottom centre of this calculation grid at various times in the relaxation process. In this figure, the director at every calculation gridpoint is represented as a cylinder. Note how the TP cholesteric layers (*a*) become distorted (*b*), and fold over (*c*, *d*) to add a twist to this small region of the display pixel. For comparison, the director configuration of the homeotropic cell at one point in the relaxation process may be seen in figure 11.

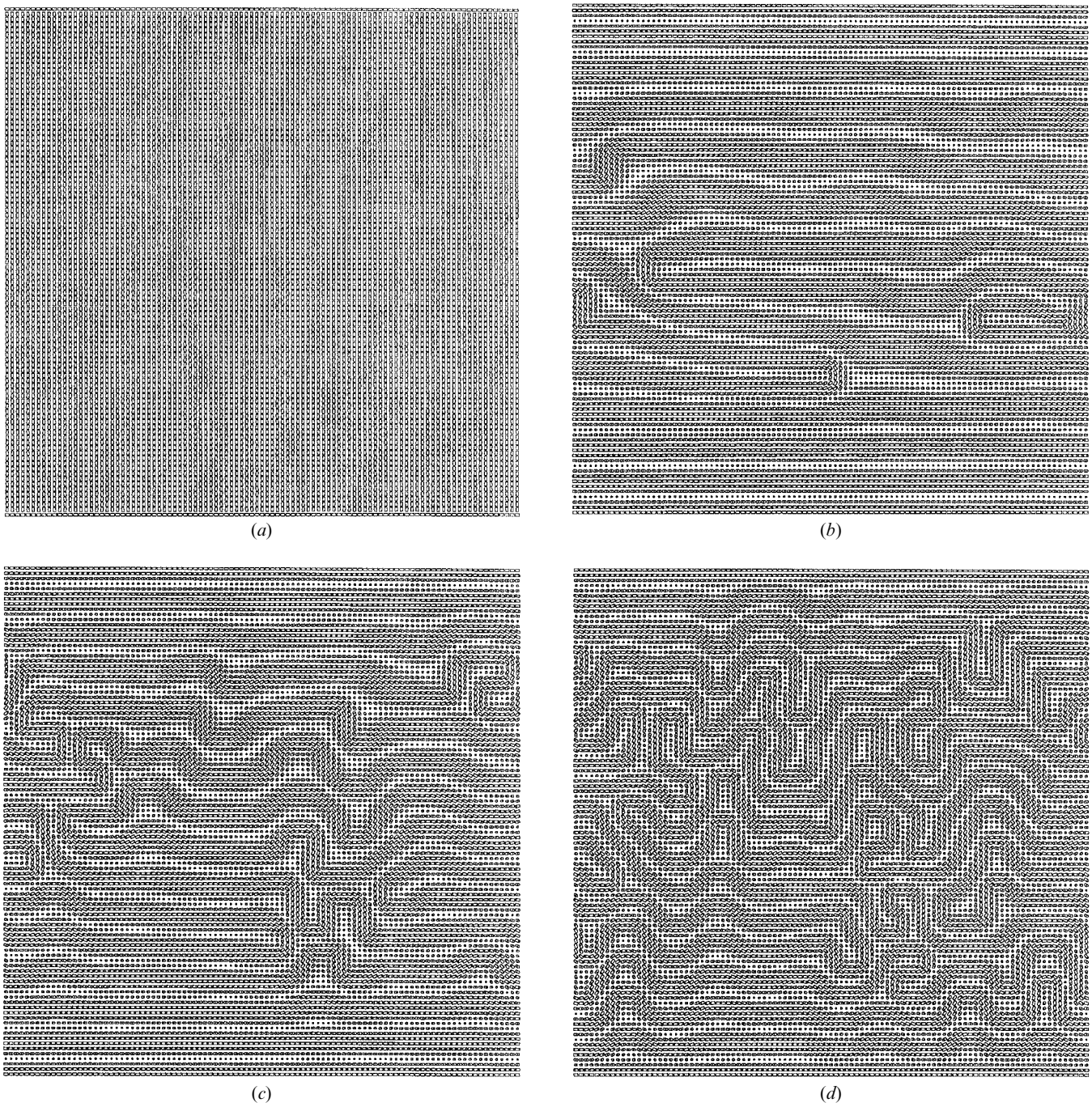

Figure 9. Simulated director configurations in relaxation from the homeotropic state to the planar state in a reflective cholesteric display with planar surfaces. These pictures represent a side view of the cell, with the top of the picture as the top substrate. (*a*) 0 ms, (*b*) 0.83 ms, (*c*) 1.67 ms, (*d*) 3.33 ms, (*e*) 8.33 ms, (*f*) 33.3 ms.

8. Simulation of optics of reflective displays

Before we may begin optical calculations, we need to have a value for the indices of refraction of our mixture. We expect that the refractive indices of the mixture may vary significantly from those of the host due to the large proportion of chiral dopant used in the experimental cell. To attempt to correct these values, weighted averages of the properties of the host and chiral dopant were used. The dielectric constants and refractive indices are not known for CB15; however, the chemical structure of CB15 is very similar to the nematic 5CB, with the exception that CB15 has a chiral centre in the alkyl chain [19]. The values of these constants have been measured for 5CB, and were used here in an average weighted by

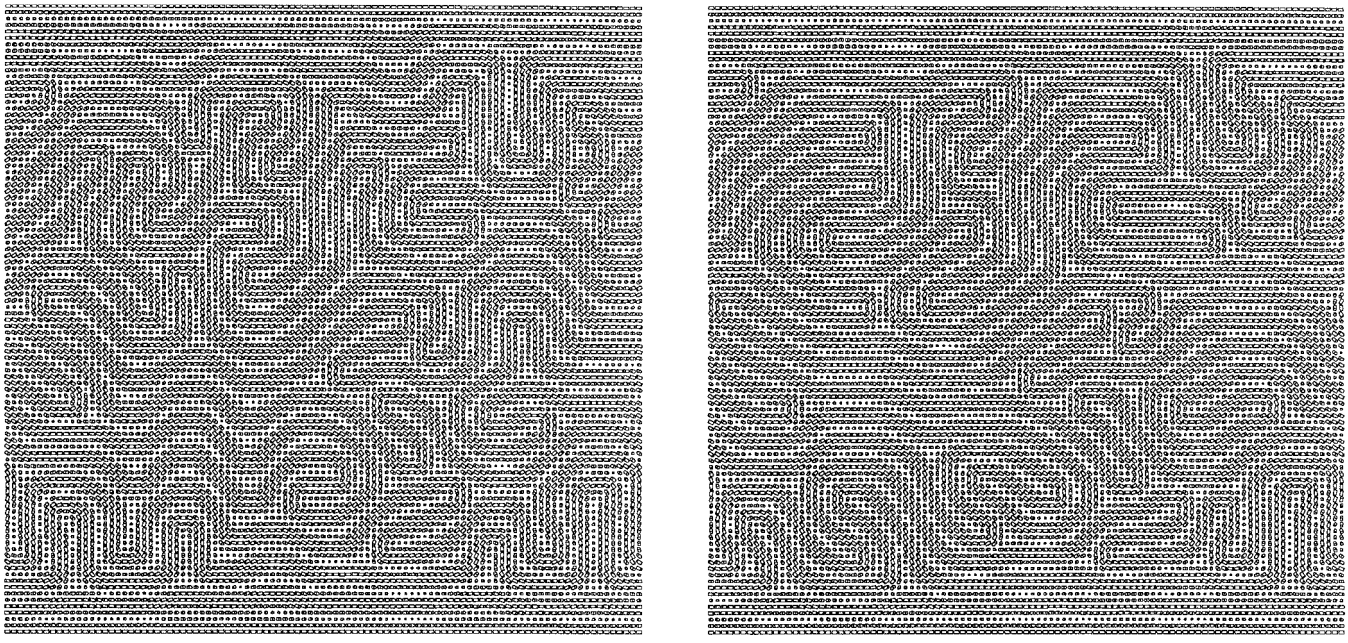

(e) (f)

Figure 9. (*Continued.*)

the percentage of that component in the system to approximate the values of the mixture. The extraordinary and ordinary indices of refraction for the nematic host are 1.7100 and 1.5076, respectively. For 5CB, the corresponding values are 1.7212 and 1.5376, yielding weighted averages of 1.715 and 1.520, respectively.

In order to reproduce plots of the reflective amplitude of the cells vs. wavelength and time at various angles of light incidence, it is necessary first to develop a method for calculating reflections from the sample. To calculate reflective optics of multi-dimensional director configurations, accurately, a full wave analysis method such as a finite difference time domain algorithm to solve Maxwell's equations in multiple dimensions is necessary [20, 21]. However, such programs are not yet commonly available. Instead, we developed a program which would convert the director configuration into a series of helical structures oriented along various axes, and determine the reflective properties of the calculated director indirectly through comparison with Berreman 4×4 calculations of reflections from helices of various degrees of twist. This technique will be described below.

Our optical simulation is based on the assumption that the director at any given time consists of regions of cholesteric helical structure and regions that are untwisted. Each helical region may be characterized by a pitch and a helical axis orientation. Light incident on a particular helical region will only be retro-reflected if its propagation direction is approximately parallel to the helical axis. The intensity of the reflection is related to the number of twists through which the light passes as it travels along the helical axis, and the relationship between the wavelength of light and the pitch of the material. By determining the effect of these parameters, we may calculate the reflectance at any given wavelength and angle of incident light from the simulated cholesteric director field.

To determine what helical components of a director configuration exist along a given incident light direction, the following procedure was implemented. First, the approximate direction of the light travel through the material was determined from Snell's law. Next, a series of light paths propagating in that direction was plotted through the calculated director field, with a light path originating at each lattice point along the $z = 0$ substrate. At every point where a light path intersected a horizontal lattice line, the approximate director at that point was determined through a linear extrapolation from the points nearest the intersection. Thus, a representation of the director field as seen by light incident at an oblique angle was obtained. In order to determine the presence of helical axes along this light direction, director elements that were not approximately perpendicular to the incident light direction were eliminated. The allowance condition for a director element to be perpendicular was that it was tilted away from the light-normal plane by less than 2°. A value of 2° was chosen because the divergence inside the material of the incident light beam of the retro-reflection apparatus was roughly 2°. This method is illustrated in figure 12.

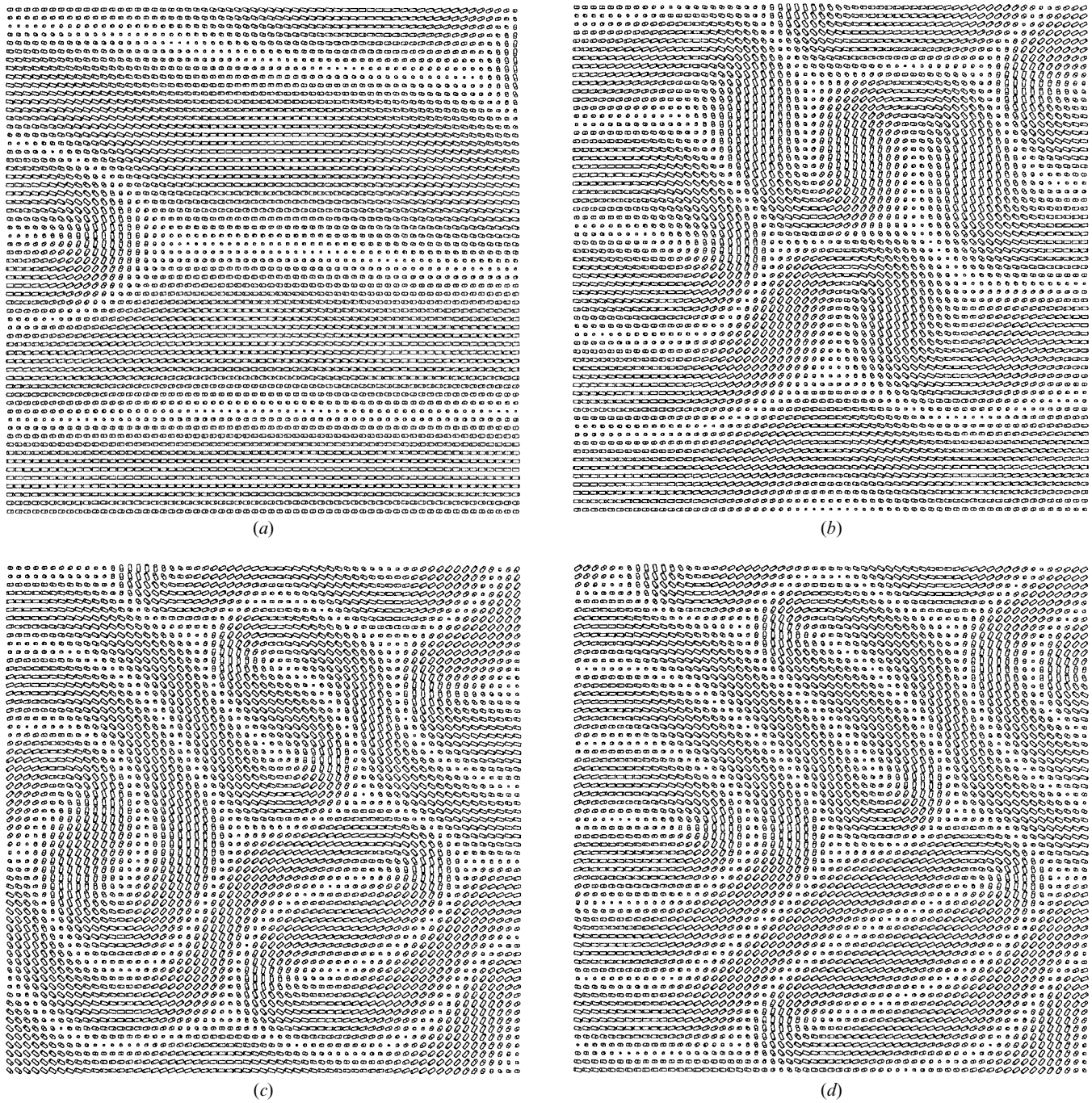

Figure 10. Magnified pictures from the homeotropic to planar relaxation simulated director configurations in relaxation from the transient planar state to the planar state in a reflective cholesteric display with planar surfaces. These pictures represent a side view of the cell, with the top of the picture as the top substrate. (*a*) 0.83 ms, (*b*) 1.67 ms, (*c*) 5.0 ms, (*d*) 10.0 ms.

With only helical components approximately parallel to the light path remaining, it was necessary to develop a method for analysing individual helices. For each helix, the pitch and degree of twist was determined from the modified director structure. Based on this pitch and twist, a distribution of reflections at various wavelengths was determined from a reference table. This table was developed by calculating the reflections at various wavelengths from cholesteric helices of varying twist using Berreman's LROPAN liquid crystal optics simulation software [22]. A plot of the reflectance curves from which the look-up table was built may be seen in figure 13. In order to compare the resulting data directly with the measured retro-reflection data from experiment,

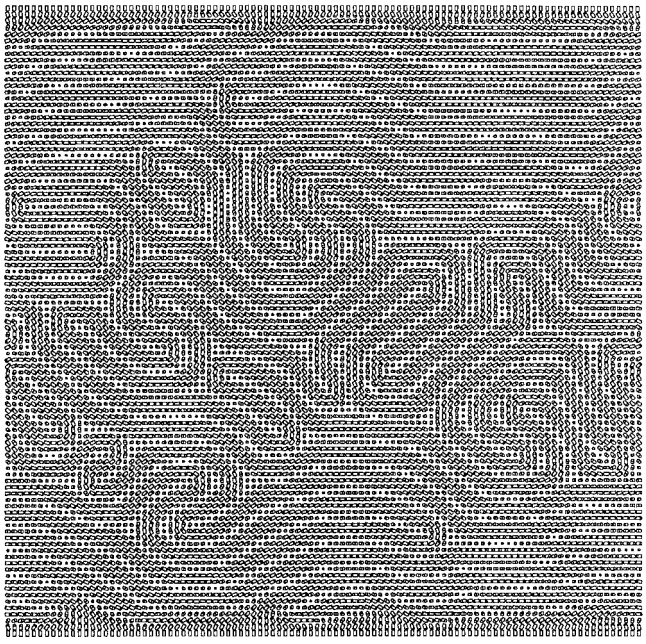

Figure 11. Simulated director configuration in relaxation from the transient planar state to the planar state in a reflective cholesteric display with homeotropic surfaces, 33.3 ms. This picture represents a side view of the cell, with the top of the picture as the top substrate.

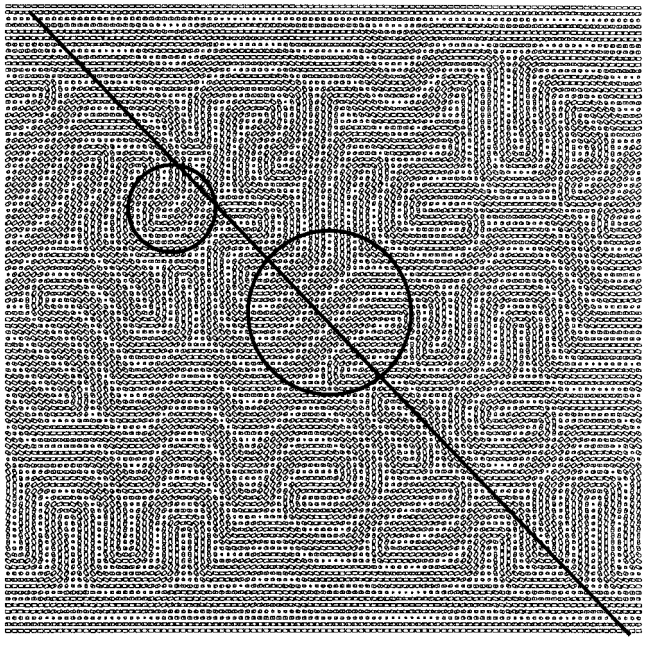

Figure 12. Schematic of optics calculation method. First, a light path is traced through the director at a chosen angle, then areas which have a periodicity along that direction are found. The pitch and number of turns of that region is determined. From these values, a reflectance can be found from a reference table.

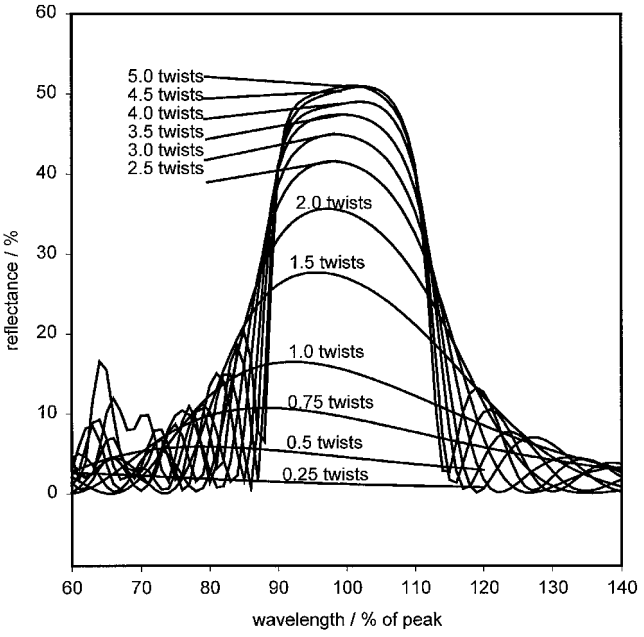

Figure 13. Spectra from which the reference table of spectra vs. number of twists at various percentages of the peak reflective wavelength was generated.

bins of width 25 nm ranging from 375 nm to 1100 nm were used. For each helix, the reflectance was determined at percentages of the central reflective wavelength, $\lambda_c = nP$, ranging from 60% of λ_c to 10% of λ_c, with the step size being 1% of λ_c. These were then placed into the appropriate 25 nm wide bins.

Once the calculated reflections of all the helices have been placed into the proper bins, a reflective spectrum of the director at the given angle of incidence can be constructed. By calculating the spectra from the simulated director configurations at various times in the relaxation process, the three-dimensional curves from experiment could be reconstructed.

9. Analysis and discussion

In the simple cholesteric system having an equilibrium state with three twists, the simulation is seen to agree very well with the observed texture. The system transformed out of the TP texture via a spatial modulation that increased in amplitude. The simulation showed that the peaks of this modulation spread out horizontally after a short time, resulting in the small regions of equilibrium twist alternating with regions of horizontal twist. It was seen in the simulation that having two regions of horizontal twist meet each other and join would result in a significant lowering of the free energy, and also result in the appearance of larger regions of equilibrium texture. These events are seen to occur in experiment, as reported earlier [7].

In order to compare the capacitance of the simulated director configurations with the experimental measurements of capacitance, it is necessary to extract a measurement of capacitance from the simulated director configurations. We may determine the average ε of the director configuration by calculating ε for each column of the director configuration and averaging, as shown in equation (4).

$$\varepsilon = \frac{1}{N_x}\sum_x \frac{1}{\frac{1}{N_z}\sum_z \frac{1}{\varepsilon_i}}, \quad \text{where} \quad \varepsilon_i = \varepsilon_\parallel \cos^2\theta + \varepsilon_\perp \sin^2\theta \tag{4}$$

In this case, N_x is the number of lattice points in the x-direction, N_z is the number of lattice points in the z direction, and θ is the angle between the director and the z-axis. From ε, it is simple to calculate the capacitance,

$$C = \frac{\varepsilon_0 \varepsilon A}{d}$$

where A is the active area of the cell, and d is the cell thickness. Figure 14 shows the calculated capacitance from the simulated director structures as a function of time for systems with homeotropic and with planar boundary conditions. Note the striking similarities between the shapes of these curves and the measured experimental curves for the two systems seen in figure 2.

Figure 15 shows the simulated retro-reflection curve for the MLC 6080 cell with the planar surface, while figure 16 shows the simulated retro-reflection curve for the cell with the homeotropic surface. Both of these calculations assume the cell to be tilted at 5° away from the incident light direction. Note the excellent agreement in the main features of the curves with the experimental data. From these calculations, it is simple to determine the wavelength of maximum reflection as a function of time. A plot showing this may be seen in figure 17.

Of particular interest is the similarity between the relaxation process observed in the simple low d/P system and the more complex high d/P system found in a real display. In both cases, on removal of voltage from the

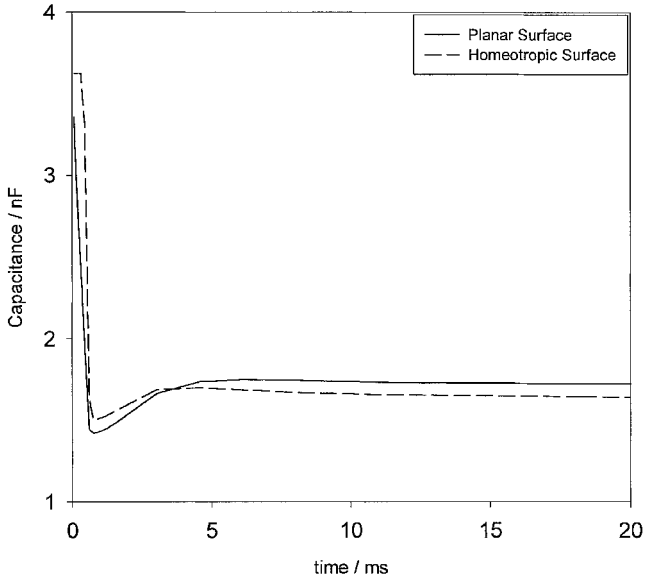

Figure 14. Simulated capacitance for cells with various surface treatments.

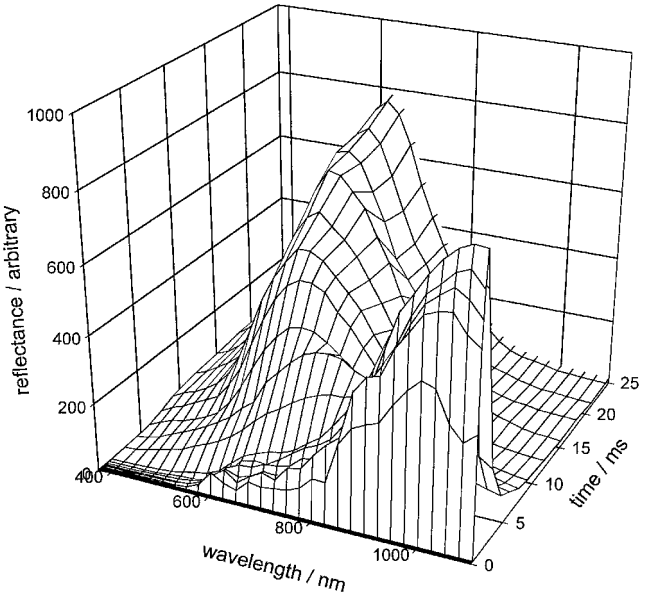

Figure 15. Simulated retroreflection data for cell with planar surfaces.

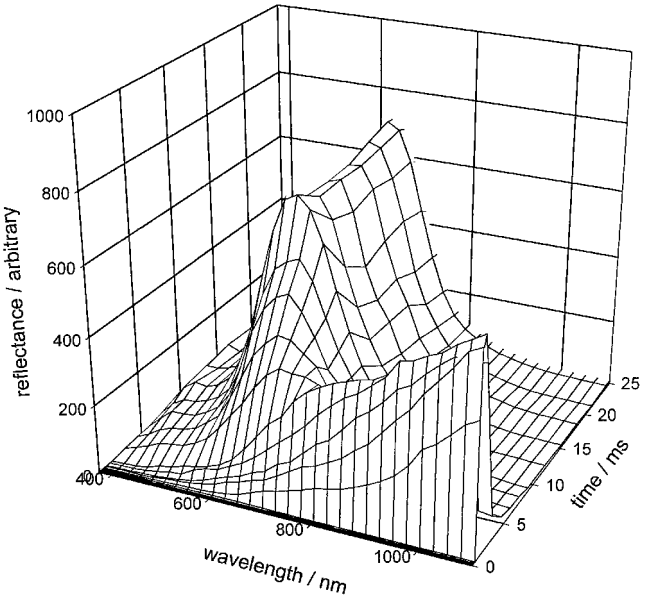

Figure 16. Simulated retroreflection data for cell with homeotropic surfaces.

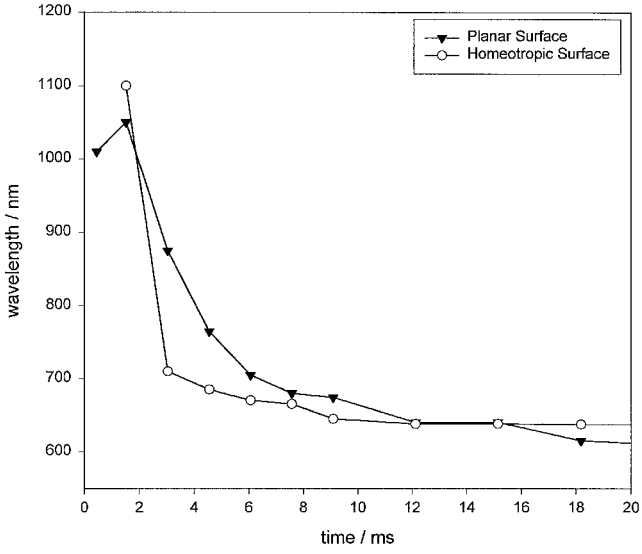

Figure 17. Simulated retroreflection data for cell with homeotropic surfaces.

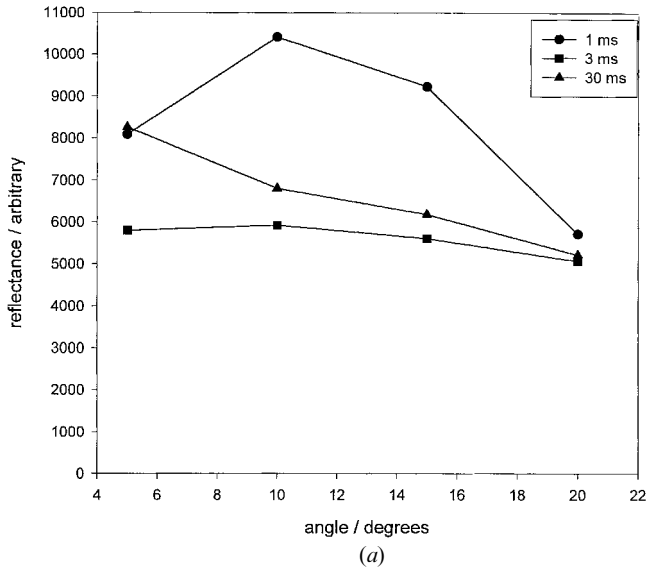

(*a*)

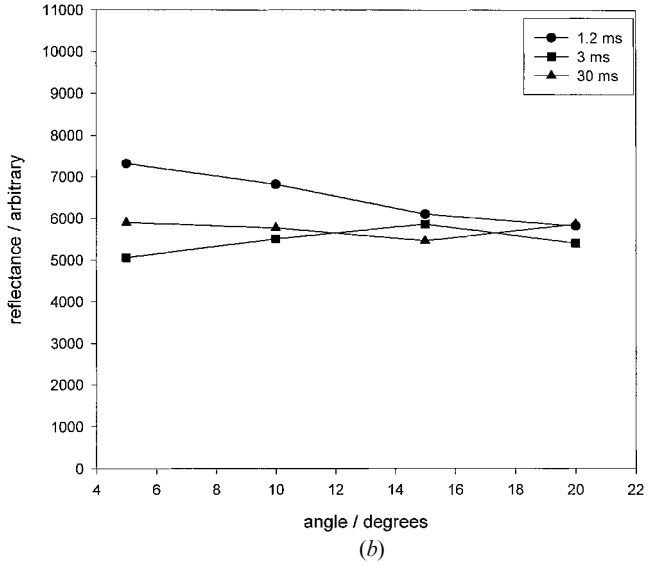

(*b*)

Figure 18. (*a*) Simulated reflectance for the planar cell at various incident angles at different times in the relaxation process. (*b*) Simulated reflectance from the silane cell at various incident angles at different times in the relaxation process.

homeotropic state, the liquid crystal relaxes to a transient planar state with a pitch significantly longer than the equilibrium pitch. Also in both cases, a modulation which is roughly sinusoidal in nature disturbs the transient planar state. By a process involving buckling and folding of cholesteric layers, the equilibrium pitch is obtained. Finally, large regions of equilibrium pitch occur as a result of movement of the domain boundaries in the simple system, and through growth of uniform domains in the more complex system.

Changes in the reflectance as a function of incidence angle α may be calculated from the simulated reflectance data in the same manner in which they were determined from the experimental data. We will only present values for $\alpha \geqslant 5°$, for ease of comparison with experiment. Figures 18 (*a*) and 18 (*b*) show these plots for the planar and homeotropic surfaces, respectively. Note how the TP reflection (at about 1 ms) at small angles is somewhat brighter than that at larger angles, as seen in the experimental data. During the transition time (3 ms), the simulated intensity takes on a much wider angular distribution. Again, as the system progresses into the P state (25 ms), the distribution for the planar cell becomes somewhat peaked at small angles, while that of the silane cell remains largely flat. It should also be noted that the relatively small area used in the simulation yields a small number of domains. In experiment a much larger statistical sample is taken. This could greatly influence the simulated helical axis distribution. Our simulations typically show less than seven full twists per angle, thus making the statistical uncertainty in the number of twists approximately $\sqrt{7}/7$ or about 40%. Due to this uncertainty, it is not surprising that the calculations of broadband reflectance as a function of angle agree only qualitatively with the experimental measurements. The performance of a large enough calculation to reduce this error significantly is impractical at the present time.

10. Summary

The validity of the simulation of the cholesteric system with $d/P = 13.9$ is suggested by the fact that the simulation qualitatively recreates all of the significant experimental observations of the transient planar to planar transition. In our earlier work [4], it was determined

that during the transition the helical axis distribution is very narrow in the transient planar state, becomes very wide in the transition time, and then becomes narrow again with increased time. Simple observation of the director structures seen in figure 9 demonstrates that simulation reproduces these effects. Additionally, the simulation recreates earlier observations on the formation and growth of domains. In the early stages of the modulation, the areas of uniform equilibrium twist are very small, figure 9 (*e*), while as time progresses they are seen to form much larger uniform regions. The size of our simulation region prohibits the growth and combination of domains beyond a size of several μm; but up to that point, the growth of domains correlates qualitatively with experimental observations published earlier [6].

In addition to such qualitative comparisons, properties derived from the simulated director configurations match very convincingly with the experimental data. We have demonstrated that the wavelength of maximum reflection changes very similarly between the simulation and experiment, and that capacitance dynamics for the simulation closely match those for experiment. Additionally, the plots of spectra vs. time for the simulated and experimental systems match very closely.

Based on these studies, we have for the first time established a complete model for the H to P transition in cholesteric liquid crystals. In this relaxation process, the materials initially is in the H state with an applied field. Upon removal of the field, the liquid crystal drops to the TP state in the plane of the cell, but with a non-equilibrium number of twists. In order to relieve the high twist energy of this state, a sinusoidal modulation forms, and after acquiring sufficient amplitude leads to a buckling and folding of the cholesteric layers, resulting in a highly distorted P state with the equilibrium pitch. Uniform cholesteric domain regions grow from this distorted cholesteric state, eventually leading to the equilibrium P state. In all points of this model, the experimental observations and computer simulations agree in a qualitative sense, and have been found to agree acceptably in quantitative measurements such as capacitance and reflection spectra.

This work was supported by NSF ALCOM grant DMR 89-20147, and DARPA N61331-96-C-0042.

References

[1] Yang, D.-K., West, J. L., Chien, L.-C., and Doane, J. W., 1994, *J. appl. Phys.*, **76,** 1331.
[2] Kawachi, M., Kogure, O., Yoshii, S., and Kato, Y., 1975, *J. appl. Phys.*, **14,** 1063.
[3] Yang, D.-K., and Lu, Z.-J., 1995, *SID'95 Dig.*, 351.
[4] Watson, P., Sergan, V., Anderson, J. E., Ruth, J., and Bos, P. J., 1999, *Liq. Cryst.*, **26,** 731.
[5] Tani, C., Ogawa, F., Naemura, S., Ueno, T., and Saito, F., 1979, *SID'79 Dig.*, 114.
[6] Sergan, V., Reznikov, Yu., Anderson, J. E., Watson, P., Ruth, J., and Bos, P. J., 1998, *Mol. Cryst. Liq. Cryst.*, **330,** 1339.
[7] Watson, P., Anderson, J. E., Sergan, V., and Bos, P. J., 1999, *Liq. Cryst.*, **26,** 1307.
[8] Helfrich, W., 1970, *Appl. Phys. Lett.*, **17,** 531.
[9] Hurault, J. P., 1972, *J. chem. Phys.*, **59,** 2068.
[10] Chigrinov, V. G., Belyaev, V. V., Belyaev, S. V., and Grebenkin, M. F., 1979, *Sov. Phys. JETP*, **50,** 994.
[11] Anderson, J. E., Watson, P., Ernst, T., and Bos, P. J., 2000, *Phys. Rev. E*, **61,** 3951.
[12] Huang, X.-Y., 1996, PhD thesis, Kent State University, USA.
[13] EOM software developed by C. Hoke, Kent State University, 1998.
[14] De Gennes, P. G., and Prost, J., 1993, *The Physics of Liquid Crystals* (New York: Oxford University Press).
[15] Berreman, D. W., 1974, *Appl. Phys. Lett.*, **25,** 12.
[16] Dickmann, S., Eschler, J., Cossalter, O., and Mlynski, D. A., 1993, *SID Dig.*, 638.
[17] Fedak, I., Pringle, R. D., and Curtis, G. H., 1982, *Mol. Cryst. liq. Cryst.*, **82,** 173.
[18] BACKFG optical software developed by D. W. Berreman.
[19] Information supplied by Merck Inc.
[20] Witzigmann, B., Regli, P., and Fichtner, W., 1998, *J. opt. Soc. Am. A*, **15,** 753.
[21] Titus, C. M., Bos, P. J., Kelly, J. R., and Gartland, E. C., 1999, *Jpn. J. appl. Phys.*, **38,** 1488.
[22] LROPAN optical software developed by D. W. Berreman.